

## 3D simulation of incompressible flow around a rotating turbulator: Effect of rotational and direction speed

ELHADI ZOUBAI<sup>a</sup>  
HOUSSEM LAIDOUDI<sup>a\*</sup>  
ISMAIL TLANBOUT<sup>a</sup>  
OLUWOLE DANIEL MAKINDE<sup>b</sup>

<sup>a</sup> University of Science and Technology of Oran Mohamed-Boudiaf,  
Faculty of Mechanical Engineering, Laboratory of Sciences and Marine  
Engineering, BP 1505, El-Menaouer, Oran, 31000, Algeria

<sup>b</sup> Stellenbosch University, Faculty of Military Science,  
Private Bag X2, Saldanha 7395, South Africa

**Abstract** This paper presents new results for the dynamic behaviour of fluid around a rotating turbulator in a channel. The turbulator has a propeller form which is placed inside a flat channel. The research was carried out using 3D numerical simulation. The rationale of the experiment was as follows: we put a propeller-turbulator inside a flat channel, and then we insert a water flow inside the channel. The turbulator rotates at a constant and uniform speed. The main points studied here are the effect of the presence of turbulator and its rotational direction on the flow behaviour behind the turbulator. The results showed that the behaviour of flow behind the turbulator is mainly related to the direction of turbulator rotating. Also, the studied parameters affect coefficients of drag force and power number. For example, when the turbulator rotates in the positive direction, the drag coefficient decreases in terms of rotational speed of the turbulator, while the drag coefficient increases in terms of rotational speed when the turbulator rotates in the negative direction.

**Keywords:** Rotating turbulator; Straight tube; Drag coefficient; Power number; Laminar flow

---

\*Corresponding Author. Email: [houssem.laidoudi@univ-usto.dz](mailto:houssem.laidoudi@univ-usto.dz)

## Nomenclature

$A$	–	frontal surface, $m^2$
$C_D$	–	coefficients of drag force
$c$	–	thickness of the core, m
$D$	–	total diameter of the propeller, m
$d$	–	diameter of the core, m
$F_D$	–	drag force, N
$J$	–	advance ratio
$H$	–	diameter of the channel, m
$N_p$	–	power number
$P$	–	dimensionless pressure
$p$	–	pressure, Pa
Re	–	Reynolds number
$T$	–	torque, J
$U, V, W$	–	dimensionless components of velocity
$u, v, w$	–	components of velocity, m/s
$u_{in}$	–	inlet velocity, m/s
$X, Y, Z$	–	dimensionless coordinates
$x, y, z$	–	Cartesian coordinates, m/s

## Greek symbols

$\mu$	–	dynamic viscosity, Pa·s
$\rho$	–	density, $kg/m^3$

## 1 Introduction

Many recent studies aim to induce geometric changes for the purpose of accelerating the flow within the channel. This dynamic behaviour can be exploited to speed up the fluid mixing process [1–3], or increase the process transferring in thermal applications [4–6]. Previous studies showed that the presence of a solid body inside a channel accelerates the movement of the flow as it passes around this body. The shape and the position of the body also play a role in the dynamic behaviour of the flow [7–10]. On the other hand, a group of researchers focused on changing the shape of the outer wall of the channel in order to develop the dynamic behavior of the fluid [11–14].

With regard to the previous work related to the subject, we mention the following: Fang *et al.* [15] studied the flow of a fluid inside a straight channel, and in order to accelerate the flow, an innovative turbulator was added inside the channel. The study included the effect of the turbulator shape. The results showed that the invented forms have a strong effect on accelerating the flow, and therefore there is a stimulation of thermal ac-

tivity. Farshad and Sheikholeslami [16] investigated the development of the stream velocity inside a canal. For this purpose, they added a turbulator whose cross-section is spiral in shape. The body is placed along the channel, and its streamlined form does not hinder the movement of the flow. The study showed that this shape helps to create a circular flow, which in turn enhances the thermal activity between the fluid and the channel. Yan *et al.* [17] studied the effect of a double tube inside a channel in order to determine its effect on the flow velocity. The study also included the impact of thermal properties on the heat transfer. It was estimated that this new design of the system can enhance the mass transfer which has a direct reflection on the heat transfer. Ebrahimpour and Sheikholeslami [18] studied the system of absorbing heat from the sun. This system relies on a straight channel placed above a thermal collector. Inside the channel, fluid passes through and absorbs energy. For the purpose of developing the fluid behaviour, a longitudinal turbulator was placed inside the channel. The study showed that the spiral shape of the turbulator causes the flow to move in a spiral manner, which increases its speed and has an increase in thermal absorption capacity of the fluid from the channel wall. Sheikholeslami *et al.* [19] inserted turbulators into a channel with the aim of strengthening the fluid's dynamic performance. This study was carried out in order to develop the thermal system of the channel, which is used in thermal exchangers related to clean energy. The new shape of these turbulators is that they contain holes, which allows for reducing the resistance of the turbulators to fluid flow, in return accelerating the flow. The results showed an improvement in the speed of the flow with significant development in thermal activity. In general, there are other works aimed at studying the shape of the inner turbulator and its spiral form on the general system of the stream [20–25].

There is also another type of turbulator, in the form of fixed rings placed in the centre of the channel. When the liquid passes around it, the flow path changes from a parallel shape to a circular shape. Among these works, we mention for example: Shafee *et al.* [26]. The shape of the ring is spiral and circular. This geometry allowed the flow to accelerate in a superior way, which effectively reflected the thermal activity of the fluid. Nakhchi *et al.* [27] and Bellos *et al.* [28] used a cylindrical turbulator that was hollow inside and had holes that allowed the liquid to pass through. That proposed form was found to have a high influence on the behaviour of the fluid.

Other researchers have combined the existence of more than two turbulators placed in parallel [29–31]. Also a positive development of the fluid

was elicited. Furthermore, there are also some works directly related to the subject under study [32–35].

It has already been noted from the previous works that the presence of a turbulator inside the straight channel increases the flow velocity, and this is what makes the thermal activity better for the fluid. Despite this, there are few works on propeller-shaped turbulators rotating at a constant speed. For this reason, this work aims to bridge this gap. In general, this paper aims to present the simulation of flow in a channel with a turbulator in the form of a propeller rotating at a constant speed. The purpose of this study is to understand the influence of both the speed of rotation of the turbulator and its direction of rotation on the dynamic and kinematic activity of the flow. This work can be used in many applications including a primarily thermal solar panel, thermal exchangers and semi-static mixers.

## 2 Physical problem and mathematical equations

The domain to be studied is described in Fig. 1. The domain is a straight channel with a propeller-turbulator rotating at a constant speed (Fig. 1a). The flow enters the channel uniformly at a constant initial velocity and exits from the other end of the channel. Fig. 1b represents the cross-section of the turbulator with the channel. The propeller-turbulator is composed of four blades and a core of diameter ( $d$ ). The total diameter of the propeller is given by ( $D$ ). Also, the diameter of the channel is given by the symbol ( $H$ ). Furthermore, Fig. 1b shows the positive direction of the propeller. Figure 1c shows the longitudinal section of the turbulator. The thickness of the core is denoted by the symbol ( $c$ ). The propeller blades are directed at an angle of  $45^\circ$ . All these channel and turbulator geometric proprieties are set in Table 1.

Table 1: Geometrical characteristics of the studied domain

$D/H$	$d/H$	$c/H$
0.65	0.25	0.5

The fluid used in this research is water, which has the following properties: density ( $\rho$ ) is  $998 \text{ kg/m}^3$ , dynamic viscosity ( $\mu$ ) is  $0.00000232 \text{ Pa}\cdot\text{s}$ . The flow entering the channel has a constant velocity determined by the Reynolds

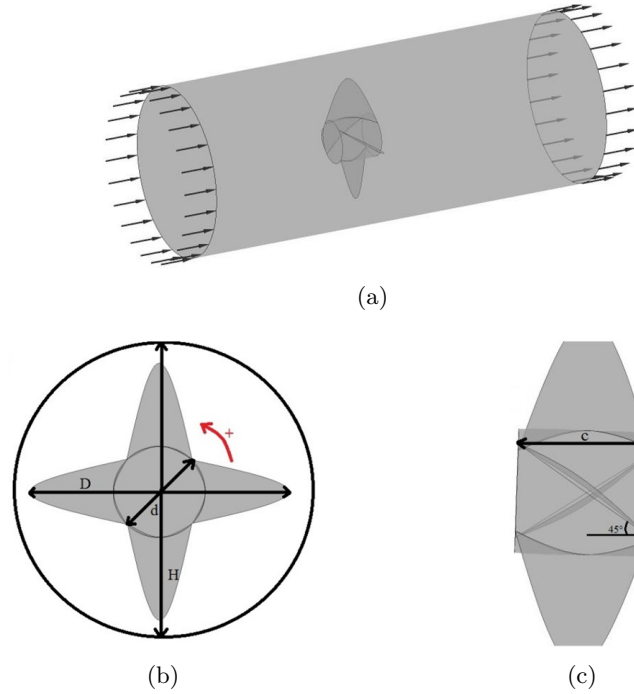


Figure 1: The studied physical domain: (a) general view of the turbulator with a channel, (b) cross-section of the turbulator, (c) longitudinal section of the turbulator.

number ( $Re = 100$ ), while the Reynolds number is given by the following expression:

$$Re = \frac{\rho u_{in} D}{\mu}, \quad (1)$$

where  $u_{in}$  denotes the velocity value at the channel entrance.

The differential equations needed to be solved to achieve numerical simulation of the problem areas follows [36–43]:

$$\frac{\partial U}{\partial X} + \frac{\partial V}{\partial Y} + \frac{\partial W}{\partial Z} = 0, \quad (2)$$

$$U \frac{\partial U}{\partial X} + V \frac{\partial U}{\partial Y} + W \frac{\partial U}{\partial Z} = -\frac{\partial P}{\partial X} + \frac{1}{Re} \left( \frac{\partial^2 U}{\partial X^2} + \frac{\partial^2 U}{\partial Y^2} + \frac{\partial^2 U}{\partial Z^2} \right), \quad (3)$$

$$U \frac{\partial V}{\partial X} + V \frac{\partial V}{\partial Y} + W \frac{\partial V}{\partial Z} = -\frac{\partial P}{\partial Y} + \frac{1}{Re} \left( \frac{\partial^2 V}{\partial X^2} + \frac{\partial^2 V}{\partial Y^2} + \frac{\partial^2 V}{\partial Z^2} \right), \quad (4)$$

$$U \frac{\partial W}{\partial X} + V \frac{\partial W}{\partial Y} + W \frac{\partial W}{\partial Z} = -\frac{\partial P}{\partial Z} + \frac{1}{\text{Re}} \left( \frac{\partial^2 W}{\partial X^2} + \frac{\partial^2 W}{\partial Y^2} + \frac{\partial^2 W}{\partial Z^2} \right), \quad (5)$$

where  $U$ ,  $V$ , and  $W$  are the dimensionless component of velocity along  $X$ ,  $Y$ , and  $Z$  directions, respectively,  $P$  is the dimensionless pressure, and  $\text{Re}$  is Reynolds number.

These equations are written in non-dimensional form after setting these variables:

$$(X, Y, Z) = \frac{(x, y, z)}{D}, \quad (U, V, W) = \frac{(u, v, w)}{u_{\text{in}}}, \quad P = \frac{p}{\rho u_{\text{in}}^2}, \quad (6)$$

where  $x, y$  and  $z$  are the directions in Cartesian coordinate system,  $u, v$ , and  $w$  are the velocity component,  $p$  is the pressure, and  $u_{\text{in}}$  is the flow velocity at the inlet.

The turbulator is characterized by a constant called the advance ratio ( $J$ ). It relates the velocity of the flow at the channel inlet to the speed of rotation of the turbulator:

$$J = \frac{u_{\text{in}}}{nD}, \quad (7)$$

where  $n$  is the rotational speed.  $J = 0.2$  to  $0.9$ . When  $J$  increases, the rotational speed of the turbulator decreases.

The power number of the turbulator can be calculated as:

$$N_p = \frac{T}{\rho n^2 D^5}, \quad (8)$$

where  $T$  is the torque. The drag coefficient of the turbulator is calculated as:

$$C_D = \frac{F_D}{0.5 \rho n^2 A}, \quad (9)$$

where  $F_D$  is the drag force exerted by the flow on the turbulator,  $A$  is the frontal surface of the propeller.

The appropriate boundary conditions for these non-dimensional equations are:

- at the inlet of the channel:

$$U = 1, \quad V = 0, \quad W = 0, \quad (10)$$

- at the channel and turbulator walls – no-slip condition:

$$U = 0, \quad V = 0, \quad W = 0, \quad (11)$$

- at the outlet tube – the Neumann condition:

$$\frac{\partial U}{\partial X} = 0, \quad \frac{\partial V}{\partial X} = 0, \quad \frac{\partial W}{\partial X} = 0. \quad (12)$$

### 3 Grid independency test and validation test

The propeller-turbulator geometry as well as the mesh were created using Gambit [44]. The number of mesh elements was set after checking its effectiveness and the results of this test are shown in Table 2. This table shows variations of the coefficient  $N_p$  in terms of mesh element number for  $J = 0.8$  and  $\text{Re} = 100$ . It is noted that the mesh of the second case of 883113 elements is very suitable for solving the above equations. We mention that the form of the mesh element is triangular. The elements are concentrated around the propeller to determine correctly the calculated results.

Table 2: Results of grid independency test

Case	Elements	Power number	Variation, %
1	441556	1.55984	2.07
2	883113	1.52743	0.23
3	1766226	1.52389	–

The numerical technique used in this research is called multiple reference frames (MRF). This technique is based on dividing the domain of computation into two main parts. The first is rotating and the second is fixed. Figure 2 illustrates this technique in the studied domain. The differential equations were solved using finite volume method (FVM). The high-resolution

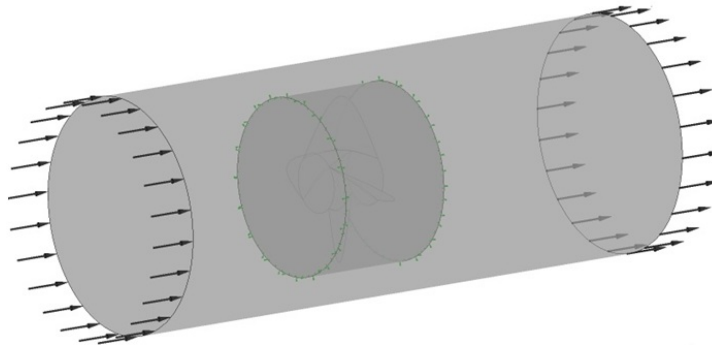


Figure 2: MRF method for the present geometry.

discretisation scheme was used for solving the convective term, whereas the SIMPLEC (semi-implicit method for pressure linked equations-consistent) algorithm was used for coupling pressure and velocity. The relative error of calculations was  $10^{-6}$  for momentum and continuity equations.

In order to validate this technique to reach accurate results, we conducted a test where we compared the results of this technique with previous research. The comparison was made with research done by Ameer and Bouzit [37]. The comparison was made on a two-bladed impeller. The values of the coefficient  $N_p$  are presented in Fig. 3 in terms of rotational speed of the mixer ( $Re$ ). Figure 3 shows that the applied technique (MRF) is very accurate in determining the results.

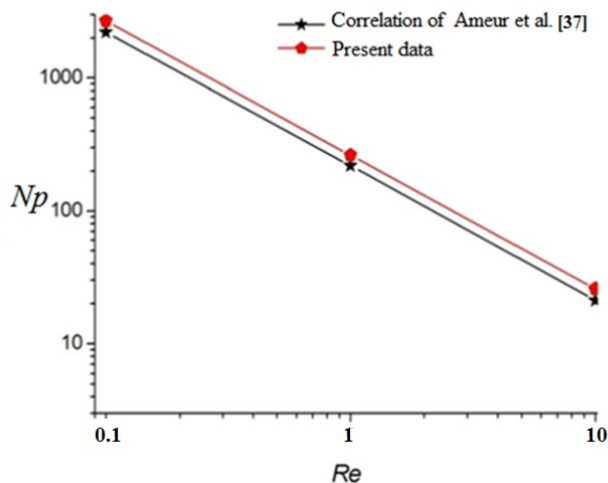


Figure 3: Validation test – comparison with the work of Ameer and Bouzit [37].

## 4 Results and discussion

Through this work, numerical experience is gathered on the effects of rotating turbulator within a tube channel. The research presents new results about the effect of rotational speed of the turbulator, as well as the direction of its rotation on flow behind the turbulator. To get an accurate understanding, numerical simulation results are presented in the form of streamlines and contours of velocity. In addition to all this, values of the coefficients  $N_p$  and  $C_D$  are presented in terms of the studied parameters.

Figure 4 shows a 3D representation of the rotating turbulator and the streamlines behind it for a constant value of the factor  $J = 0.7$ . Figure 4 shows the effect of the direction of rotation of the turbulator on the hydrodynamic behaviour of the fluid in the back. It is clearly noticed that the direction of the rotation greatly affects the performance of the turbulator, that is, the flow motion in the first case (positive direction) is more circular compared to the second case (negative), and this is a result of the shape of the turbulator blades.

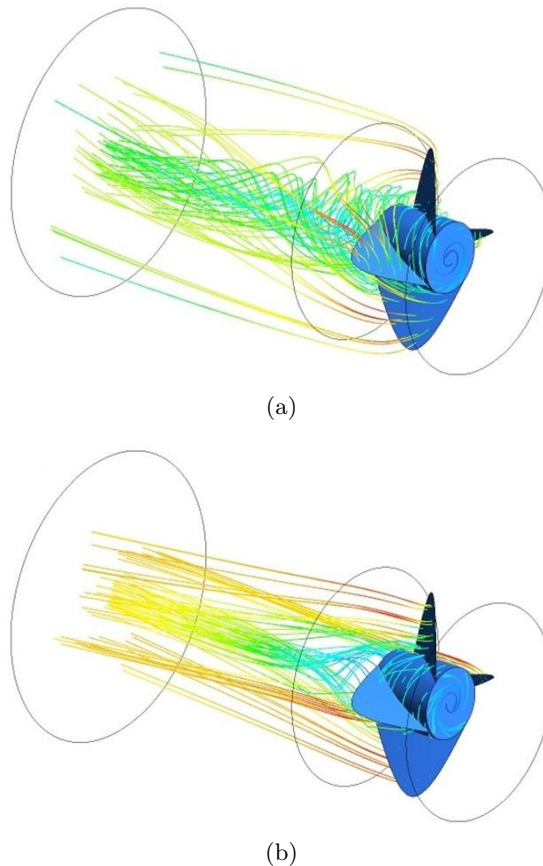


Figure 4: Streamlines behind the turbulator for  $J = 0.7$ : (a) turbulator rotates in the positive direction, (b) the turbulator rotates in the negative direction.

Figures 5 and 6 illustrate the streamlines of several cross-sections of the tube. The first section is before the turbulator; the second is located just behind the turbulator; the third section is after the turbulator. The purpose

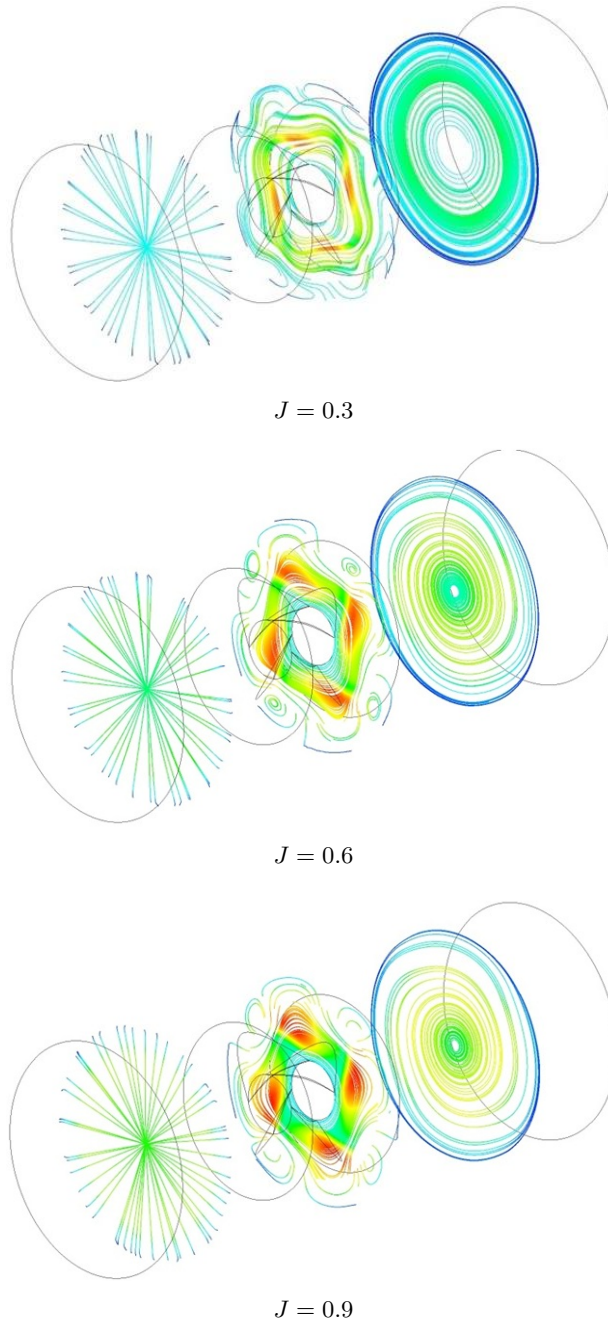


Figure 5: Two-dimensional streamlines for the positive rotational direction of the turbulator for different values of  $J$ .

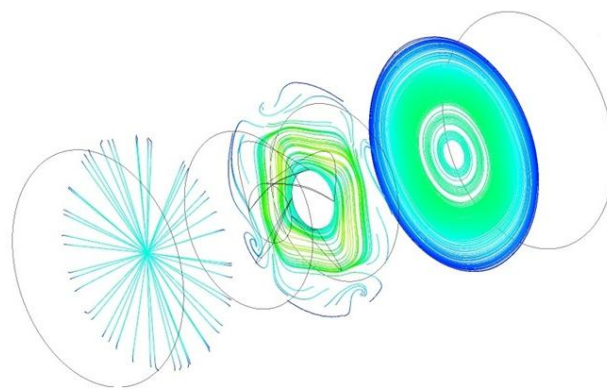
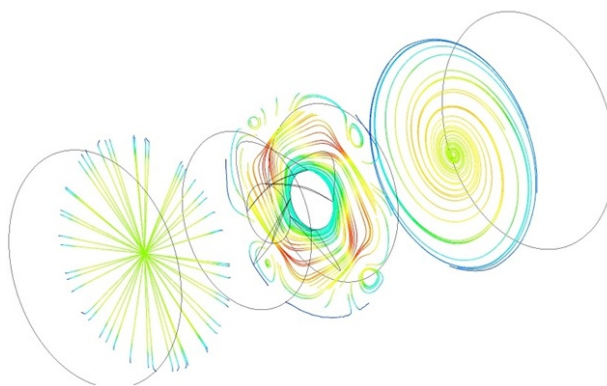
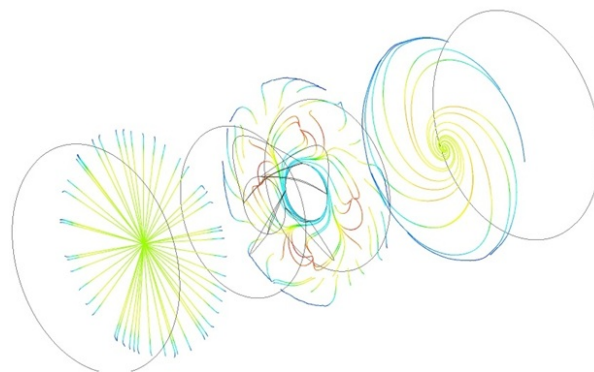
 $J = 0.3$  $J = 0.6$  $J = 0.9$ 

Figure 6: Two-dimensional streamlines for the negative rotational direction of the turbulator for different values of  $J$ .

of these figures is to understand exactly the behaviour of the flow along the tube, i.e. before and after the turbulator. Figure 5 is for the positive rotation of the turbulator. Meanwhile, Fig. 6 is for the negative direction. We also mention that the higher the value of factor  $J$ , the rotational speed of the turbulator is decreased. The two figures show that the dynamic behaviour of the flow is divided into three main parts. The first part is before the turbulator, and here the flow is stable and regular. The second part is near the turbulator from the back side, and here we notice that the flow changes its regular pattern to a circular pattern due to the circular movement of the turbulator. In this section, we notice a large vortex inside the section with small vortices near the inner wall of the tube. The reason for the formation of small vortices is due to the difference in pressure between the ends of the turbulator blades (four small vortices for four blades). In the third part, the flow becomes purely rotational, having only a main vortex. Moreover, through the third section, we can deduce the direction of the flow motion and the turbulator as well.

Figures 7 and 8 show contours of dimensionless velocity along the channel. The longitudinal view of these figures was taken in the middle of the channel. The figures show the effect of direction of rotation of the turbulator and the effect of rotational speed on the local distribution of flow velocity. It is noticed in all cases that the maximum value of the velocity is located at the turbulator sides. For the first case (Fig. 7), the values of velocity behind the turbulator increase with a gradual increase in the rotational speed of the turbulator. For the second case (Fig. 8), the values of velocity behind the turbulator remain almost constant with the increasing rotational speed of the turbulator. Furthermore, in both cases, the higher the rotational speed of the turbulator, the lower the value of the maximum flow velocity at the turbulator side. In general, it is noted that the flow velocity increases significantly after passing through the turbulator. In addition, the flow velocity values are higher when the turbulator rotates in the positive direction.

Figure 9 represents the variation of the power number ( $N_p$ ) in terms of the factor  $J$  and the direction of rotation of the turbulator. This coefficient indicates the mechanical power required for the turbulator to rotate. It is well shown that in the first case, the rotation of the turbulator creates a thrust for the propeller in the opposite direction to the flow entering the channel, so it is noted that the values of the power number are much larger as compared to the second case. Also, the values of this number increase with the decreasing rotational speed of the turbulator in the first case.

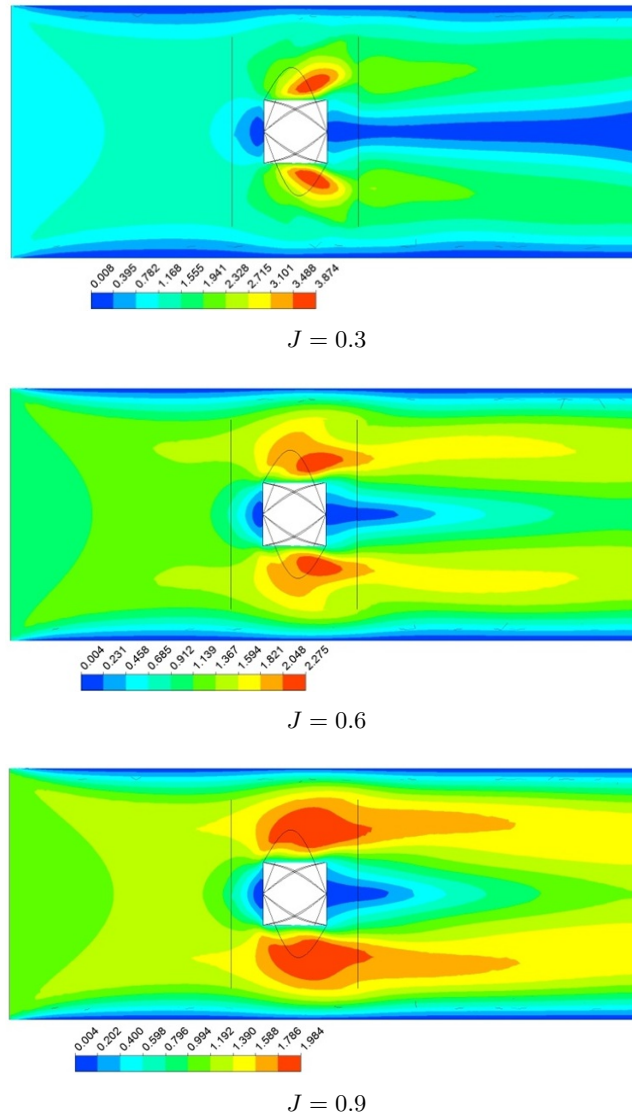


Figure 7: Contours of dimensionless velocity for the positive rotational direction of the turbulator for different values of  $J$ .

On the other hand, in the second case, the resulting thrust is in the same direction as the flow, so the values of the power number is lower. Also, there is a different trend in the relationship as compared to the first case. There is a maximum value of  $N_p$  when  $J$  takes the value of 0.6.

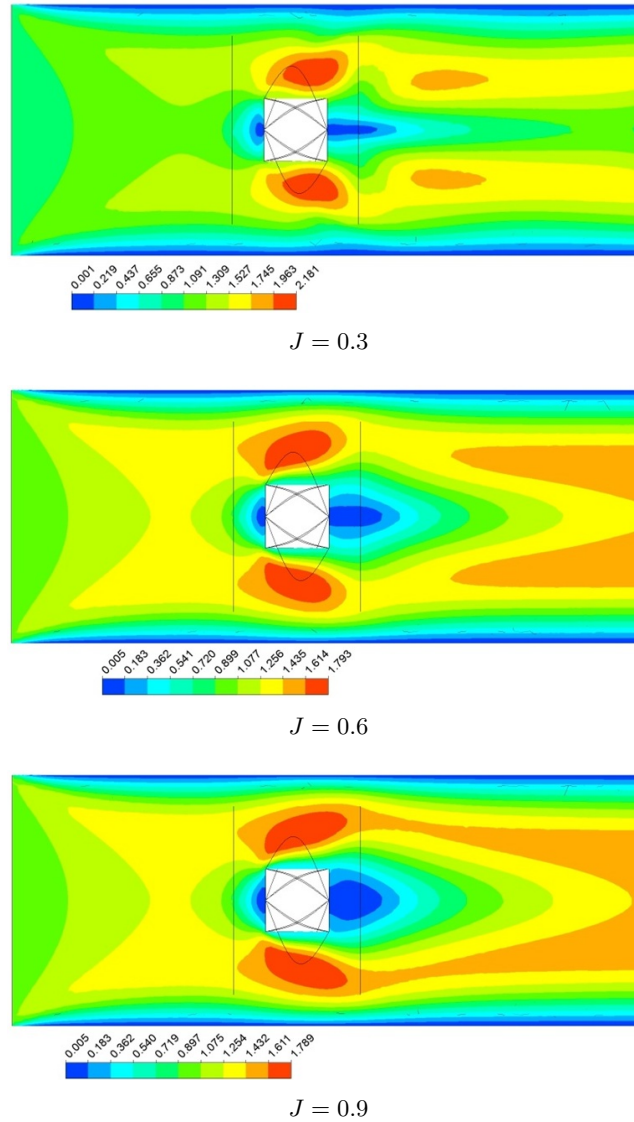


Figure 8: Contours of dimensionless velocity for the negative rotational direction of the turbulator for different values of  $J$ .

Figure 10 presents the variation of the drag coefficient in terms of factor  $J$  and direction of the turbulator rotation. Obviously, the values of this coefficient in the first case are greater than in the second case. In addition to this, in the first case, the higher the value of factor  $J$ , the lower the

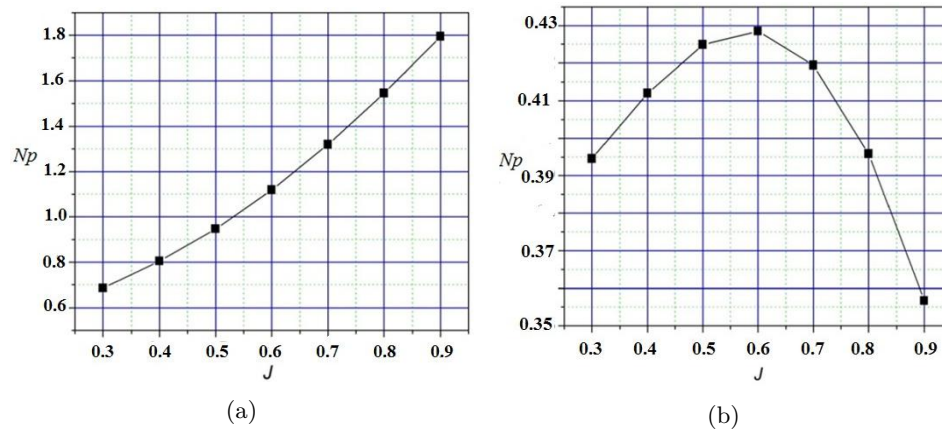


Figure 9: Variation of power number ( $N_p$ ) of the turbulator *versus*  $J$ : (a) for the case of positive direction, (b) for the case of negative direction.

value of drag coefficient, while in the second case, the decrease in the rotational speed of the turbulator increases the value of this coefficient. This shows that in the first case, the thrust force of the turbulator is in the direction opposite to the flow motion, while in the second case, the thrust force of the turbulator is in the same direction as the flow entering the tube.

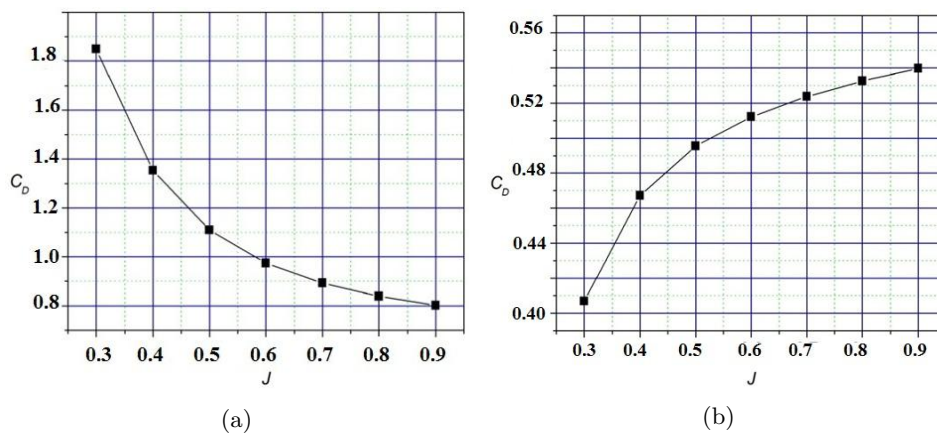


Figure 10: Variation of drag coefficient ( $C_D$ ) of the turbulator *versus*  $J$ : (a) for the case of positive direction, (b) for the case of negative direction.

## 5 Conclusions

In this work, we performed a numerical simulation of a marine turbulator inside a straight channel. The purpose of this study was to understand the hydrodynamic behaviour of flow in this case. The elements studied here are the speed and direction of rotation of the turbulator, while the velocity of the flow entering the channel is constant and determined in terms of the Reynolds number equal to 100. The main points drawn from this work are:

- The turbulator rotation in the first case (positive rotation) creates an opposite thrust to the direction of flow entering the channel.
- The thrust force of the turbulator in the second case (negative rotation) has the same direction as the flow motion.
- The dynamic behaviour of the water inside the channel is divided into three main parts: the first part extends from the entrance of the canal to the end of the turbulator; the second part is from the back of the turbulator a little backwards, then the third part begins where the flow motion becomes perfectly circular.
- It was concluded that the presence of the rotating turbulator in the canal accelerates the flow and makes the velocity higher near the canal wall.
- With regard to the effect of rotation direction, it was found that when the turbulator rotates in the positive direction, a higher flow is produced near the canal wall compared to the negative direction.

*Received 16 February 2023*

## References

- [1] Ameer H.: *Agitation of yield stress fluids in different vessel shapes*. Eng. Sci. Technol. Int. J. **19**(2016), 1, 189–196.
- [2] Laidoudi H.: *Hydrodynamic analyses of the flow patterns in stirred vessel of two bladed impeller*. J. Serb. Soc. Comput. Mech. **14**(2020), 2, 117–132.
- [3] Mishra V.P., Kumar P., Joshi J.B.: *Flow generated by a disc turbine in aqueous solutions of polyacrylamide*. Chem. Eng. J. **71**(1998), 1, 11–21.
- [4] Acharya N.: *Magnetized hybrid nanofluid flow within a cube fitted with circular cylinder and its different thermal boundary conditions*. J. Magn. Magn. Mater. **564**(2022), 2, 170167.

- [5] Laidoudi H., Bouzit M.: *The effect of asymmetrically confined circular cylinder and opposing buoyancy on fluid flow and heat transfer*. Defect Diffus. Forum **374**(2017), 18–28
- [6] Dawar A., Acharya N.: *Unsteady mixed convective radiative nanofluid flow in the stagnation point region of a revolving sphere considering the influence of nanoparticles diameter and nanolayer*. J. Indian Chem. Soc. **99**(2022), 10, 100716.
- [7] Goldanlou A.S., Sepehirad M., Papi M., Hussein A. K., Afrand M., Rostami S.: *Heat transfer of hybrid nanofluid in a shell and tube heat exchanger equipped with blade-shape turbulators*. J. Therm. Anal. Calorim. **143**(2021), 1689–1700.
- [8] Saleh B., Sundar L.S., Aly A. A., Ramana E. V., Sharma K. V., Afzal A., Abdelrhman Y., Sousa A.C.M.: *The Combined effect of  $Al_2O_3$  nanofluid and coiled wire inserts in a flat-plate solar collector on heat transfer, thermal efficiency and environmental  $CO_2$  Characteristics*. Arab. J. Sci. Eng. **47**(2022), 9187–9214.
- [9] Rani P., Tripathy P.P.: *Heat transfer augmentation of flat plate solar collector through finite element-based parametric study*. J. Therm. Anal. Calorim. **147**(2022), 639–660.
- [10] Laidoudi H., Helmaoui M., Bouzit M., Ghenaïm A.: *Natural convection of Newtonian fluids between two concentric cylinders of a special cross-sectional form*. Therm. Sci. **25**(2021), 5, 3701–3714.
- [11] Zaboli M., Ajarostaghi S.S.M., Saedodin S., Kiani B.: *Hybrid nanofluid flow and heat transfer in a parabolic trough solar collector with inner helical axial fins as turbulator*. Eur. Phys. J. Plus. **136**(2021), 841.
- [12] Oleiwi A., Mohsen A. M., Abdulkadhim A., Abed A.M., Laidoudi H., Abderrahmane A.: *Experimental and numerical study on the heat transfer enhancement over scalene and curved-side triangular ribs*. Heat Transf. **52**(2023), 5, 3433–3452.
- [13] Ramla M., Laidoudi H., Bouzit M.: *Behaviour of a non-newtonian fluid in a helical tube under the influence of thermal buoyancy*. Act. Mech. Auto. **16**(2022), 2, 111–118.
- [14] Acharya N.: *Spectral quasi linearization simulation of radiative nanofluidic transport over a bended surface considering the effects of multiple convective conditions*. Eur. J. Mech. B-Fluid. **84**(2020), 139–154.
- [15] Fang Y., Mansir I.B., Shawabkeh A., Mohamed A., Emami F.: *Heat transfer, pressure drop, and economic analysis of a tube with a constant temperature equipped with semi-circular and teardrop-shaped turbulators*. Case Stud. Therm. Eng. **33**(2022), 101955.
- [16] Farshad S.A., Sheikholeslami M.: *FVM modeling of nanofluid forced convection through a solar unit involving  $MCTT$* . Int. J. Mech. Sci. **159**(2019), 126–139.
- [17] Yan S.R., Golzar A., Sharifpur M., Meyer J. P., Liu D.H., Afrand M.: *Effect of U-shaped absorber tube on thermal-hydraulic performance and efficiency of two-fluid parabolic solar collector containing two-phase hybrid non-Newtonian nanofluids*. Int. J. Mech. Sci. **185**(2020), 105832.
- [18] Ebrahimpour Z., Sheikholeslami M.: *Intensification of nanofluid thermal performance with install of turbulator in a LFR system*. Chem. Eng. Process. Proc. Intensific. **161**(2021), 108322.

- [19] Sheikholeslami M., Abohamzeh E., Jafaryar M., Shafee A., Babazadeh H.: *CuO nanomaterial two-phase simulation within a tube with enhanced turbulator*. Powder Technol. **373**(2020), 1–13.
- [20] Farshad S.A., Sheikholeslami M.: *Nanofluid flow inside a solar collector utilizing twisted tape considering exergy and entropy analysis*. Renew. Energ. **141**(2019), 246–258.
- [21] Sheikholeslami M., Ebrahimpour Z.: *Thermal improvement of linear Fresnel solar system utilizing  $Al_2O_3$ -water nanofluid and multi-way twisted tape*. Inter. J. Therm. Sci. **176**(2022), 107505.
- [22] Khetib Y., Sait H., Habeebullah B., Hussain A.: *Numerical study of the effect of curved turbulators on the exergy efficiency of solar collector containing two-phase hybrid nanofluid*. Sustain. Energ. Technol. Assess. **47**(2021), 101436
- [23] Aghaei A., Enayati M., Beigi N., Ahmadi A., Pourmohamadian H., Sadeghi S., Dezfulizadeh A., Golzar A.: *Comparison of the effect of using helical strips and fines on the efficiency and thermal-hydraulic performance of parabolic solar collectors*. Sust. Energ. Technol. Assess. **52**(2022), 102254.
- [24] Yang L., Du K.: *Thermo-economic analysis of a novel parabolic trough solar collector equipped with preheating system and canopy*. Energy **211**(2020), 118900.
- [25] Farshad S.A., Sheikholeslami M.: *Simulation of nanoparticles second law treatment inside a solar collector considering turbulent flow*. Physica A **525**(2019), 1–12.
- [26] Shafee A., Arabkoohsar A., Sheikholeslami M., Jafaryar M., Ayani M., Nguyen-Thoi T., Basha D.B., Tlili I., Li Z.: *Numerical simulation for turbulent flow in a tube with combined swirl flow device considering nanofluid exergy loss*. Physica A **542**(2020), 122161.
- [27] Nakhchi M.E., Hatami M., Rahmati M.: *Effects of CuO nano powder on performance improvement and entropy production of double-pipe heat exchanger with innovative perforated Turbulators*. Adv. Powder Technol. **32**(2021), 8, 3063–3074.
- [28] Bellos E., Tzivanidis C., Tsimpoukis D.: *Enhancing the performance of parabolic trough collectors using nanofluids and turbulators*. Renew. Sust. Energ. Rev. **91**(2018), 358–375.
- [29] Sheikholeslami M., Farshad S.A., Said Z.: *Analyzing entropy and thermal behavior of nanomaterial through solar collector involving new tapes*. Int. Comm. Heat Mass Transf. **123** (2021), 105190.
- [30] Sheikholeslami M., Ali Farshad S., Shafee A., Babazadeh H.: *Influence of  $Al_2O_3$  nano powder on performance of solar collector considering turbulent flow*. Adv. Powder Technol. **31**(2020), 9, 3695–3705.
- [31] Sheikholeslami M., Farshad S. A.: *Nanoparticles transportation with turbulent regime through a solar collector with helical tapes*. Adv. Powder Technol. **33**(2022), 3, 103510.
- [32] Mustafa J., Alqaed S., Sharifpur M.: *Numerical study on performance of double-fluid parabolic trough solar collector occupied with hybrid non-Newtonian nanofluids: Investigation of effects of helical absorber tube using deep learning*. Eng. Anal. Bound. Elem. **140**(2022), 562–580.

- [33] Dovom A.R.M., Aghaei A., Joshaghani A.H., Dezfulizadeh A., Kakavandi A.A.: *Numerical analysis of heating aerosol carbon nanofluid flow in a power plant recuperator with considering ash fouling: a deep learning approach*. Eng. Anal. Bound. Elem. **141**(2022), 75–90.
- [34] Afshari F., Sozen A., Khanlari A., Tuncer A.D., Sirin C.: *Effect of turbulator modifications on the thermal performance of cost-effective alternative solar air heater*. Renew. Energ. **158**(2020), 297–310.
- [35] Abu-Hamdeh N.H., Bantan R.A.R., Khoshvaght-Aliabadi M., Alimoradi A.: *Effects of ribs on thermal performance of curved absorber tube used in cylindrical solar collectors*. Renew. Energ. **161**(2020), 1260–1275.
- [36] Mokeddem M., Laidoudi H., Makinde O.D., Bouzit M.: *3D simulation of incompressible Poiseuille flow through 180° curved duct of square cross-section under effect of thermal buoyancy*. Period. Polytech. Mech. Eng. **63**(2019), 4, 257–269.
- [37] Ameer H., Bouzit M.: *Power consumption for stirring shear thinning fluids by two-blade impeller*. Energy **50**(2013), 326–332.
- [38] Hassouni S., Laidoudi H., Makinde O. D., Bouzit M., Haddou B.: *A qualitative study of mixing a fluid inside a mechanical mixer with the effect of thermal buoyancy*. Arch. Thermodyn. **44**(2023), 1, 105–119.
- [39] Seddik-Bouchouicha M., Laidoudi H., Hassouni S., Makinde O.D.: *Study of the effect of geometric shape on the quality of mixing: examining the effect of length of the baffles*. Arch. Thermodyn. **44**(2023), 2, 69–85.
- [40] Bulat P.V., Volkov K.N.: *Fluid/solid coupled heat transfer analysis of a free rotating disc*. Arch. Thermodyn. **39**(2018), 3, 169–192.
- [41] Szymanski P., Mikielwicz D.: *Challenges in operating and testing loop heat pipes in 500-700 K temperature ranges*. Arch. Thermodyn. **43**(2022), 2, 61–73.
- [42] Cyklis P.: *Heat transfer in falling film evaporators during the industrial process of apple juice concentrate production*. Arch. Thermodyn. **39**(2018), 3, 3–13.
- [43] Aliouane I., Kaid N., Ameer H., Laidoudi H.: *Investigation of the flow and thermal fields in square enclosures: Rayleigh-Bénard’s instabilities of nanofluids*. Therm. Sci. Eng. Prog. **25**(2021), 100959
- [44] Gambit. <http://www.gambit-project.org/> (accessed 11 Aug. 2022).